Multi-Body Dynamic Modeling and Simulation of Crawler-Formation Interactions in Surface Mining Operations -Crawler Kinematics

Samuel Frimpong[1]

[1] Missouri University of Science and Technology

Received: 7 February 2015 Accepted: 28 February 2015 Published: 15 March 2015

Abstract

Surface mining operations use large tracked shovels to achieve economic bulk production capacities. Shovel reliability, maintainability, availability and efficiency depend on the service life of the crawlers. In rugged and challenging terrains, the extent of crawler wear, tear, cracks and fatigue failure can be extensive resulting in prolonged downtimes with severe economic implications. In particular, crawler shoe wear, tear, cracks and fatigue failures can be expensive in terms of maintenance costs and production losses. This research study is a pioneering effort for understanding and providing long-term solutions to crawler-formation problems in surface mining applications. The external forces acting on the crawler shoes and oil sand are formulated to determine system kinematics. The dynamic model focuses on the external force from machine weight, the crawler contact forces, the contact friction forces and the inertia and gravity forces using multi-body dynamics theory. A virtual prototype simulator of the crawler dynamics is simulated within the MSC ADAMS environment.

Index terms— surface mining, crawler-terrain interactions, multi-body dynamic theory, crawler dynamic modeling, virtual prototype simulation.

1 Introduction

able shovels are widely used in surface mining operations. The lower works of this shovel comprise propel and crawler systems, which

2 C

The crawler tracks are made up of shoes that are connected together by link pins to form a continuous chain [2]. Multi-body dynamics study on crawler-terrain interactions is non-existent for large shovels in surface mining operations but it is required to provide knowledge of crawler performance and fatigue life. Fatigue life modeling and analysis are also required to develop preventive maintenance plans, component replacements and rebuilds to extend the life of the crawlers and reduce their maintenance costs. Nakanishi and Shabana (1994) used a 2-D hydraulic excavator model to study the multi-body dynamics of a tracked vehicle. The track interaction with sprockets, rollers and ground were modeled using the spring-damper force to calculate the track-terrain normal contact forces. The tangential force was modeled using a simple Coulomb friction model. Choi et al. (1998) and Lee et al. (1998) extended the 2-D study of Nakanishi and Shabana (1994) to a 3-D contact force models of a hydraulic excavator. Rubinstein and Hitron (??004) used an LMS-DADS simulation to develop a multi-body dynamic M113 armored carrier tracked vehicle simulator. Hertz theory was used to model the track-terrain contact force, and user-defined force elements to calculate normal and tangential forces between the track and the terrain. ??ubinstein and Coppock (2007) extended this model by including grousers in the track-terrain model. Ferretti and Girelli (1999) developed a 3-D dynamic model of an agricultural tracked vehicle using

Newton-Euler rigidbody theory. They introduced a track-terrain model using soil mechanics theory to generate the dynamics of the system. They used these parameters as input in the dynamic model to calculate sinkage and shear displacement of the track. Ryu et al. (2000) developed a computational method for a non-linear dynamic model of military tracked vehicle. They used compliant force elements between the pins and track links to increase the degrees of freedom (DOF) based on the track-terrain contact force model by Choi et al. (1998). Madsen (2007) used MSC ADAMS to simulate a complex tracked hydraulic excavator. The model used the contact force model in ADAMS to define the crawler-terrain interactions. **??**a and Perkins (1999) developed a hybrid track model for a large mining shovel crawler using continuous and multibody track model. A commercial multi-body dynamics code, DADS, was used to assemble the continuous and multi-body track vehicle model. Their study was limited to studying a 2-D dynamic contact between track and sprocket during the propel motion.

Previous research on multi-body dynamic models has also focused on shovel dipper-bank interactions. Frimpong et al. (2005) used an iterative Newton-Euler method to develop a dynamic model of boom, dipper handle and dipper assembly. Their dynamic model identified the important factors that determine the performance of the shovel during its digging phase. Frimpong and Li (2007) also modeled the interaction between the dipper of a cable shovel and oil sands formation using multi-body dynamics theory. In addition, the shovel boom was made flexible to determine its deformation and stress distribution during shovel operations.

Frimpong and Thiruvengadam (2015) have formulated the kinematics of the crawler-flexible terrain interactions of a large mining shovel in surface mining operations (P&H 4100C BOSS Electric Shovel in Figure 1). They showed that 132 DOFs in the crawler-terrain system are driven by external forces and dynamic analysis is required to generate the remaining DOFs. This paper advances the kinematic models to formulate the dynamic models for the crawler-terrain interactions based on the rigid multi-body dynamics theory **??**14, 15, 16 and 17].

3 II.

4 Rigid Multi-body Dynamics of Crawler-Terrain Interactions

Figure 2 illustrates the geometry of the crawler track assemblies for the P&H 4100C Boss shovel. The track is modeled using the crawler track dimensions given in Table 1. Only the open track chain of the crawler assembly, in contact with the ground (Figure 1), is used for this study. Since the crawler track is made up of crawler shoes, a simplified crawler shoe model is developed first and then connected together to form the multi-body model of track assembly. This simplified model is generated in Solidworks based on the actual crawler shoe model for P&H 4100C Boss shovel [18]. The mass moment of inertia of each body in the system used for the dynamic analysis **??**19, 20 and 21] is obtained directly from MSC ADAMS. The crawler shoes 2-14 are identical and all of them have the same mass moment of inertia about their centers of mass.

5 III.

6 Dynamic Equations of Motion

The shovel weight (W), supported by two crawlers, is uniformly distributed on the crawler shoes that are in contact with the ground [2]. This study Figure 3 : Ground Forces acting on the shovel crawler track ground for one crawler track. This crawler track segment along with one half of the vehicle load (W/2) acting on it is shown in Figure 3. From Wong (2001), when the vehicle sinks vertically to the ground the ground exerts normal force (FN), and tangential force (FT) (longitudinal and lateral) on the crawler track segment as shown in Figure 3. These normal and tangential forces are modeled using inbuilt contact force mechanism in MSC ADAMS.

Crawler shoes dynamic equilibrium for link i: In the multibody model shown in Figure 2, the weight is assumed to be equally shared by thirteen crawler shoes. The uniformly distributed load applied on each shoe is in addition to its self-weight. The mass of the crawler shoe is assumed as mi. The free body diagram of a crawler shoe i with inertia forces in dynamic equilibrium with external and joint constraint forces is shown in Figure **?? ??**14, 22 and 23]. The external forces acting on the crawler shoe # i are the gravity force (mig) due to selfweight of the shoe, uniformly distributed load (wi) due to machine weight and contact forces due to the interaction between crawler shoe and ground as shown in Figure 3. The joint forces are due to reactive fo rces at the spherical joints and and parallel primitive joints and as shown in Figure **??**.

The following dynamic equation of motion uses the notations and formulation described in Shabana [14,15]. The dynamic equations of motion for the constrained rigid body i using centroidal body coordinate system from Shabana [14,15] is given by equation (1).

focuses only on the crawler shoes in contact with the(W/2) (w i) (? ? ? , ? ? ?) (? ? ??1,? , ? ? ??1, ? ? ?,?+1 , ? ? ?,?+1) (? ? ??1,? , ? ? ??1,? ? ? ?,?+1 , ? ? ?,?+1) i c i e i v i i Q Q Q q M ? ? ? ? ? ? (1)

i = 2, 3,?,14 for crawler shoes and i = 15, 16,?,64 for oil sand units.

7 Generalized Inertia Forces of Crawler shoe i = 2, 3,?,14:

The generalized inertia force is given by the left hand side of the equation 1. From Shabana [14,15] (F ?,3 ?,?+1 , ? ?,3 **??**) is the unit vectors along the x, y, z axis of the centroidal coordinate system of body and inertia tensor **??**14, 22 and 23] of shoe i in its centroidal coordinate system aligned with global coordinate system shown in

Figure 2. Equation (**??**) is the angular velocity vector in the body coordinate system.?,?+1 Z X Y C C I ? ? ? ? ? ? ? ? ? ? ? ? ? Q Q i v i v 0 = of generalized acceleration of body I (4)**(5)**T i i i i i i i] ? ? R R R [z y x ? ? ? ? ? ? ? ? ? ? ? ? ? ? ? ? ? ? q = ? ? ? ? ? ? ? ? ? ? ? ? ? ? i i i i m m m 0 0 0 0 0 0 m RR (6) (7) i i i i G I G m ?? T ? ?? ? ? ? i v Q = ? ?] [T ? G I ? I ? G ?? ?? ? ? i i i i i i ? ? ? (9) i i i ? G ? ? ?i i i i i i i i ? ? ? ? ? ? ? G Equation (

Generalized External Forces acting on crawler shoe i = 2, 3,?, 14: The first term on the RHS of equation (1) gives the generalized external forces in the crawler track multi-body system [14]. The distributed load on each crawler shoe is due to the weight of the machine. The total machine load, excluding the weight of the crawler shoes in contact with the ground, is assumed to be distributed uniformly on each crawler shoe as shown in Figure **??**. For example, the total machine weight [1] is 1,410,184 kg. Half of this weight is 705,092 kg. The total number of crawler shoes in contact with the ground (for the P&H 4100C BOSS) is 16, and thus, the total weight of 16? ? ? ? ? ? ? ? ? ? ? ? ? ? ? e R e e Q Q Q i i i

is the vector of generalized applied forces associated with the translation coordinates is the vector of generalized applied forces associated with the orientation coordinates (?).

The gravity force, distributed machine load, and contact forces are the external forces acting on the crawler system. The generalized external forces are obtained from Shabana [14,15].

The self-weight of the crawler shoe due to its mass acting at its centroid C is shown in Figure **??**. The mass of the crawler shoe from Table 1 4681.67 kg and the gravity force acting at the center of mass of each crawler shoe = 432.3 KN. The gravi ty force vector) acting on each crawler shoe i in the global coordinate system = The generalized forces, associated with the gravity force, are given as equations (12) and (**??**3).

() (13) (14) ? ? R i e Q R); ? ? ? i e Q (m) i = ? i m g m i = i g F) ? ? T i g m ? 0 0 ? g m i i g i 0 0 Q Q Q i z i y i x F Q R ? ? i g T i i i i F G u A Q C ? 0 0 0 ~i c i c i c i c i c i c i C**12**

x y x z y z u is a transformation matrix given in Frimpong and Thiruvengadam (2015); equation (**??**4) is a skew symmetric matrix associated with the vector is the position vector of center of mass of body i with respect to the origin of the body coordinate system. Since the origin of the reference point of body i coincide with the center of the .w i g i d F ? ? T i g w ? 0 0 (15) ? g w Q Q Q i i i z i y i x i 0 0 d R F Q

mass of body i, the vector =0.Therefore, These generalized forces are added to the generalized external force vector in equation (1). 0 ? i ? Q . i e Q i C

Contact force between crawler shoe and ground: Figure **??** also shows the 3-D contact forces (normal and tangential) and the torque between track shoe i and ground **??**21, 24 and 25]. These forces will act on the crawler shoe bottom surface at a point I [28] as shown in Figure **??**. The normal force ( )shown in Figure 6 is calculated using the impact function model in MSC ADAMS. In this model, when two solid bodies come in contact with each other a nonlinear spring damper system is introduced to determine the normal force **??**26, 27, 28 and 29]. (17) kstiffness of the spring = penetration depth = distance variable used in the impact function model; and e -force exponent = 2.0. maximum damping coefficient = and d -penetration depth at which maximum damping is applied = 0.0001 m. The normal force vector acting at point I for the crawler shoe i is

The coulomb friction model in Adams is used for calculating tangential frictional force)shown in Figure 6. Based on this model, the frictional force acting at point I is calculated based on equation (**??**8) **??**21, 25, 28 and 29]. (18) = friction coefficient defined as a function of slip velocity vector at contact point I [28,29]. The friction parameters listed in Table 2 are used in the study for calculating tangential forces. ? ? i d T i i d i i F G u A Q ? ? ?

is the position vector of point of application of equivalent force with respect to the origin of the body coordinate system. These generalized forces are added to the generalized external force vector in equation (1). given by The components of the tangential forces and are calculated by substituting ? obtained from friction coefficient-slip velocity relationship into equation 18 [28,29]. The friction torque about the contact normal axis shown in Figure 6 impedes any relative rotation of shoe i with respect to the ground [29]. This torque is proportional to the friction force [29].? ? T i d i d i d i d z y x ? u i d F i e Q F N ? ? ? ? ? ? ? ? ? ? 0 if 0 0 if) 1 , , 0 , 0 , (Step * max x x d x x c kx e i N ? F m N/ 10 1 8 ? ; x - max c - m s N / 10 1 4 ? ? ? ? T z N y N x N i N F F F , , , ? F i N s i T F V F) (? ?) (s V ?] [, , , z s y s x s s V V V ? V (F T Static Friction Coefficient (µ s) Dynamic Friction Coefficient (µ d) Static Transition velocity (V st , m) Dynamic Transition velocity (V d , m) 0.4 0.3 0.01 0.1? ? z T y T x T i T F F F , , , ? F x T F , , y T F , z T F , i T i T F (19) i T i RF T**3**

2 ? R = radius of the contact area [29]. The generalized forces associated with contact force vector at point I and torque from Shabana (2010).i T i N i I F F (F ? ?) i T (20) (21)

Generalized External Forces acting on Oil sand unit i = 15, 16,?, 64: The contact forces, and spring damper unit i as shown in Figure 7. The crawler shoes exert equal and opposite contact forces

) and frictional torque) on oil sand unit i at point J as in Figure 7. Consequently, the generalized forces associated with contact force vector and friction torque on oil sand unit i is given by equations (22) and (**??**3).

(? z T z N y T y N x T x N i I i z i y i x i F F F F F F Q Q Q , , , , , , F Q R ? ? i T i i i I T i i I i i T G A F G u A Q) (~? ? ? ?

is the position of contact point I on body i with respect to the coordinate system. The generalized forces are added to the generalized external force vector in equation (**??**)? ? T i I i I i I i I z y x ? u i e Q i J (F i (T i J

F i T i I i J i F F Q R ? ? ? ? ? i T i i i J T i i J i i T G A F G u A Q) (~? ? ? ? = position of contact point J on unit i

with respect to the body coordinate system shown in Figure 7. In addition to the contact force, two springdamper forces are also exerted on the oil sand unit as shown in Figure 7. This spring damper force acts along the line connecting points and on oil sand unit i to corresponding points and on default ground link of MSC Adams (Figure 7). The spring damper force acting along the line connecting points and from Shabana (2010) can be expressed as in equation (**??**4). (**??**4)? ? T i J i J i J i J z y x ? u? ? 1 1 1 , l c l l k F o s ? ? ? ?

k -spring stiffness; c -damping constant; -length of spring 1 at any time -undeformed spring length; -time derivative of and the spring coefficient, damping coefficient and length are listed in Table 3. The generalized forces associated with spring force can be derived from Shabana (2010) as in equations (**??**5) and (26) In equation (29), is the vector of system kinematic constraint equations (both joint and driving constraints) and ? is the corresponding vector of system Lagrange multipliers. The number of Lagrange multipliers in the vector ? = total number of constraint equations in thevector = = 346 or 347 as defined in kinematics part of this paper. Substituting the expression for into equation (**??**), the equation of motion for part i is given by equation (**??**0). ? ?,1 ? ?,2 ? ?,1 ? ?,2 1 , s F ? ?,1 ? ?,1 1 1 t; l o l ? l 1 ; l oij P s i F 1 , 1 , 1 , r Q R ? ? ? ? ij P T i i P i s i F 1 , 1 , 1 , 1 , r G u A Q ? ? 1 1 , 1 , ?lij P ij P r r ? = 1 , s F

unit vector along the line of action of force? ij P 1 , r j P i P 1 , 1 , r r ? i 1 , P r j 1 , P r ? ?,1 ? ? i P i P i P i P z y x 1 , 1 , 1 , 1 , ? u? ?,1 i i ? C Q q T i i c ? ?) , (t q C C ?) , (t q C n c i c Q i v i e i i Q Q ? C q M T q i ? ? ? ? ? (i = 2, 3, 4, ??**, 64)**

For = 63 interconnected rigid multi-body system shown in Figure 2, the differential equations of motion can be written from Shabana (2010) as in equation (**??**1).

(31) (32)

The total number of differential equations in equation (**??**1) is = 378, while the number of unknowns are the sum of = 378 generalized accelerations and = 346 or 347 Lagrange multipliers. From Shabana (2010), the additional nc equations needed to solve for n + nc unknowns are obtained from kinematic constraint acceleration equation defined in Frimpong and Thiruvengadam (2015) and by equation (33). Equations (**??**1) and (33) can be combined and can be expressed in matrix form as in equation (**??**4).

(33) (34) v e T q Q Q ? C q M ? 64 3 2 M 0 0 M M M ? ; ? ? ? ? ? ? ? ? ? ? ? ? ? ? ? ? ? ? T q T q T q T q C C C C 64 3 2 ? ; ? ? ? ? ? ? ? ? ? ? ? ? ? ? ? ? 64 3 2 e e e e Q Q Q Q ? ; and ? ? ? ? ? ? ? ? ? ? ? ? ? ? ? 64 3 2 v v v v Q Q Q Q ? d q Q q C ? d v e q T q Q Q Q q C C M ? ? ? 0

The above system of differential algebraic equations is solved numerically using MSC ADAMS to predict motion parameters and reaction forces. is the position of contact point on oil sand unit i with respect to its body coordinate system. Similarly, the generalized forces can be derived for the spring damper-2 system shown in Figure 7. These generalized forces are added to the generalized external force vector I e Q in equation (1).

8 IV. Solutions to the Dynamic Equations

9 ? ?,1

Generalized Constraint Forces acting on crawler shoe and oil sand unit i: The crawler shoe is connected to crawler shoe -1 and +1 by four joints (two spherical and two parallel primitive joints) as shown in Figure **??**. Similarly an oil sand unit i is connected to four adjacent oil sand units by two spherical joints and two inplane primitive joints as defined in the kinematics part of this paper. The generalized constraint forces are obtained using Lagrange multipliers (?) defined in Shabana [14,15] and can be expressed in general form as in equation 29.

i comparing the analytical results with the numerical results obtained by solving the same problem with MSC ADAMS. A two-body dynamic problem in which a rectangular block whose dimensions and mass properties are within the same order of magnitude as the crawler shoe is assumed to slide on a flat rectangular terrain. The flat terrain is in turn fixed to the ground. The rectangular block and flat plane interact through contact forces. The objective of this problem is to determine the generalized accelerations, joint reaction forces and driving constraint forces analytically for given initial conditions at time t, as shown in Figure 8.

In this multi-body system, the flat plane and rectangular block are labelled as body 2 and body 3 in Figure 8. respectively. The global and centroidal body coordinate systems are also shown in Figure 8. The dimension of the flat terrain is 30m x 1m x 10m and that of the rectangular block is 0.5m x 0.5m x 3.5 m. The densities of rectangular block and flat terrain are assumed to be same as the density of crawler shoe (Table 1) This two-body system has twelve absolute Cartesian coordinates. The vector of system generalized coordinates from Shabana (2010) is expressed as in equation (35). The absolute velocity vector can be written as equation (36). At time t = 0, the system generalized coordinates and velocity vector are defined by equations (**??**7) and (38).

() (36) (37) (38)**35**

Body 2 is fixed to the ground using fixed joint as shown in Figure 8 and has zero degrees of freedom. The position and orientation of the centroidal coordinate system of body 2 shown in Figure 8 are fixed with respect to the global coordinate system. The six constraint equations for body 2 can be written as equation (39) from Shabana (2010). ? ? T T] R R R R R R R [3 3 3 3 z 3 y 3 x 2 2 2 2 z 2 y 2 x 3 2 ? ? ? ? ? ? ? ? ? q q q T] R R R R R R [3 3 3 3 z 3 y 3 x 2 2 2 2 z 2 y 2 x ? q T t] 0 2 / 0 25 . 0 0 .

5 25 . 3 2 / 2 / 2 / 3 5 . 0 5 0 . 15 [ ) 0 (? ? ? ? ? ? ? ? q T t] 0 0 0 0 0 0 0 0 0 0 0 0 [ ) 0 (? ? q ? 0 2) , (**0 2**)? t C t C t C R t C R t C R t C z y x q q q q q q

The constraint equations for body 2 can be written in a vector form as equation (40) and the corresponding vector of Lagrange Multipliers as equation (**??**1).

(40) (41) ? ? ? ? ? ? ? ? ? ? ? ? ? ? ? ? ? ? T t C t C t C t C t C t C t , , , , , , , 6 5 4 3 2 1 2 q q q q q q q C ? ? ? T ? ? ? ? ? ? ? 6 5 4 3 2 1

10 ? ?

Body 3 is constrained to move in the x-direction with a constant velocity of 0.5 m/s without changing its orientation. But it can move freely in z and y-directions. The required driving force is assumed to act at the centroid of body 3. The four driving constraint equations for body 3 are given by equation (42). The vector of constraint equations for body 3 is given by equation (43) and the corresponding vector of Lagrange multipliers is also given by equation (**??**4). The free-body diagram of flat plane (Body 2) and rectangular block (Body 3) is shown in Figures 9 and 10. Due to fixed joint constraints (Figure 9), the orientation of body 2 coordinate system vector with respect to the global coordinate system at any time is equal to the initial orientation at 0 t = 0. Thus, the time rate of change of is also equal to zero. ? ? ? ? ? ? ? ? ? ? ? ? ? t C t C t R t C

x q q q The vector of system constraint equations and Lagrange multipliers are given by equations (**??**5) and (46). There are twelve absolute coordinates and ten constraint equations and hence the degree of freedom for this simple system is two. q q q q q q q q q q q q C ? ? ?] [(44) ? ? T ? ? ? ? 10 9 8 7 3 ? ? ? ? ? ? ? ? ? ? ? T t t t , , , 3 2 q C q C q C ? or ? T t C t C t C t C t C t C t C t C t C t C t ,? ?? t C q (43) ? ? ? ? ? ? ? ? ? ? ? ? ? T t C t C t C t C t , ,, **, , 10 9 8 7**

3 q q q q q C ? Similarly due to driving constraints the orientation of the body 3, does not change with time . Therefore , for any given time . Since T] [3 3 3 3 ? ? ? ? ? ? ? ? ? ? T t t] 0 2 / 0 [0 3 3 ? ? ? ? ? ? ? ? ? t 3 ? is . fixed with respect to time ? ? T t] 0 0 0 [3 ? ? ? ? .

The mass inertia matrix of body 2 and body 3 are given in Table **??**.

Table **??** : Mass and Inertia tensor of Body 2 and Body 3

The rectangular block (body 3) sinks vertically to the ground (body 2) and hence The values of the penetration ( ) and penetration velocity ( ) in equation (**??**7) to calculate normal force) and slip velocities ( ) in equation (**??**8) to calculate tangential forces ( ) at any time t are obtained by simulating the schematic model in Figure 8 in MSC ADAMS. These values are shown in Table 5 for t = 0.5s. The friction parameters used in the tangential force calculation are listed in Table 6. It can be seen from Table 5 that the tangential forces since slip velocities in y and z directions, ? ? y N x N F F . x x) x s V T F 0 , , ? ? z T y T F F 0 , , ? ? z s y s V V .

Normal Force (N) The contact force vector on body 2 is equal and opposite to that of body 3 as shown in Figure 9 ( ).

The data used to obtain mass matrix , Jacobian of the kinematic constraints , generalized external forces and generalized quadratic velocity ve ctor in equation (**??**1) for body 2 and body 3 are listed in Table 7.

i.e. 7 and are substituted in to equation 34 and solved for and . The results are listed in Tables 8 and 9.3 2 I J F F ? ? M q C e Q e QM 2.340E6 0 0 0 0 0 0 2.340E6 0 0 0 0 0 0 2.340E6 0 0 0 0 0 0 1.9503E8 0 0 0 0 0 0 1.75718E8 0 0 0 0 0 0 1.96975E7 T e 2 Q 0 0 -23002618 0 5091625 0 2 q C 1 0 0 0 0 0 0 1 0 0 0 0 0 0 1 0 0 0 0 0 0 1 0 0 0 0 0 0 1 0 0 0 0 0 0 1 0 0 0 0 0 0 0 0 0 0 0 0 0 0 0 0 0 0 0 0 0 0 0 0 T v 2 Q 0 0 0 0 0 0**Body**

] [3 2 q q q C C C ? 0 Q ? d 0 Q ? d q ? ? ? Table 8 : Solution for ? ? ? ? ? 2 (m/s 2) ? ? ? 2 (m/s 2) ? ? ? 2 (m/s 2) ? ? 2 (d/s 2) ? ? 2 (d/s 2) ð ??" 2 (d/s 2) ? ? ? 3 (m/s 2) ? ? ? 3 (m/s 2) ? ? ? 3 (m/s 2) ? ? 3 (d/s 2) ? ? 3 (d/s 2) ð ??" 3 (d/s 2) 0 0 0 0 0 0 0 0 -3.3236521 0 0 0

11 Generalized Constraint Forces

Using the vector ? in Table 9, the generalized constraint forces for body 2 and body 3 is given by equation (47) from Shabana (2010). These force values are listed in Table 10.

(47)

12 Generalized Constraint Forces

13 Actual Fixed Joint Forces on body 2

The actual reaction forces where and are joint reaction forces and moments in the global x, y, and z directions at the fixed joint (point K) shown in Figure 9 for body 2 can be found using generalized constraint forces . From Shabana (**??**010 ? ? ? ? ? ? ? ? ? ? ? ? ? T T T c T c T T T c T c] 0 0 [ ] [10 9 8 7 3 3 3 c 6 5 4 3 2 1 2 2 2 c ? ? ? ? ? ? ? ? ? ? ? ? ? ? ? ? ? ? ? R ? R Q Q Q Q Q Q ? ? T R c Q (N) ? ? T c ? Q (N-m)? ? T 2 2 2 M F R ? 2 F 2 M ? ? ? ? ? ? ? ? ? ? ? ? ? ? ? ? ? ? T T T K K K c T c K T z y x R c T z y x M M M F F F 2 2 2 2 2 2 2 2 1 2 2 2 2 2 2 2 2 2 2 2 2 2 and 5 . 0 0 . 5 0 . 15 , G A G u u A u Q G Q u M Q F ? R ? ? ? ? ? ? ? ? ? ? ? ? ? ? ?

14 Actual Driving Forces on body 3

Similarly the actual driving forces where and are driving forces and moments at point D for body 3 (Figure 10) can be obtained from the generalized driving constraint forces3 .? ? T 3 3 3 M F D ? 3 F 2 M 3 c Q . From Shabana (2010), (49) ? ? T F F F 3 3 3 ? ? 3 Q ? ? ? ? ? ? ? ? ? ? 3 1 3 3 3 3 3 3 3 c T R c D T z y x M M M Q G Q u M ? ? ? ? ? ? ? 0 u A u ? ? 3 3 3 D D since, ? ? T D 0 0 0 3 ? u and ? ? T T 3 3 3 G A G ? Table 10 :

The fixed joint and driving forces are tabulated in Table 11.

15 Table 11 : Joint and Driving Forces

The comparison between analytical and simulated values from Adams is summarized in Table 12. The table 12 shows the generalized accelerations on body 2 and body 3, actual reaction forces and moments due to fixed joint on body 2 and driving forces and moments on body 3 at time t = 0.5 s. It can be seen from Table 12, the absolute value of maximum error between the analytical solution and Adams simulated results is within 2%. Hence Adams can be used with confidence for simulating complex multi-body dynamic simulation problems.

Table 12 : Comparison between Analytical and MSC Adams results at t = 0.5s

The differential algebraic equations (DAE) for the complex crawler-formation interaction given in equation (34) are solved in MSC ADAMS using GSTIFF integrator with I3 formulation [29]. The GSTIFF is a variable-order, variable-step, multi-step integrator based on backward difference formula (BDF). It has maximum integration order of six to calculate solution for the first order ODE's using multi-step predictor-corrector method. The solution methodology for the GSTIFF integrator described below follows the procedure defined in MSC Adams/Solver user manual [29]. In Adams the equations of motion in equation (**??**4 z (N-m) 0 0 0 0 0 0 q C q q, Q ? C q M T q ? ? ?) , ( ) , (t t ? ? ?

To use GSTIFF integrator equation (**??**0) is converted to first order ODE by introducing a new velocity variable in equation (**??**0). This substitution results in equation (51).0 q C 0 q u 0 u q, Q ? C u q M T q ? ? ? ? ? ?) , ( ) , ( ) (t t ? ? (51)

The index of the DAE is defined as the number of time derivatives required to convert DAEs to a system of ODEs [29]. The equation (**??**0) or (**??**1) is in the default Index 3 (I3) formulation of GSTIFF integrator. Equation (51) can also be written in the form of equation (**??**2)q u ? ? [29] (52) 0) y F(y ? t , , ?

In equation (52) state vector Predictor Step: An explicit predictor step is used to obtain the initial guess value of vector at current time in equation (52). In this step, Taylor seriesT] [? q, u, y ? . 1 ? n y 1 ? n t

polynomial of given order is fitted using the past values of vector y to obtain1 ? n y .

Corrector Step: The corrector equation for the state vector y at the current time can be obtained from backward difference formula [29] as shown in equation (53).

Using equation (53), equation (**??**6) can be derived as follows:

(56) Adams (specified error = 1.0E-003), the solver proceeds to the next time step. Otherwise the integrator takes a smaller time step and recalculates the solution. This predictor-corrector process is repeated until the simulation end time is reached.? 0 0 0 0 q q q qq q u C I C Q ? C u M Q y F T T ? and ? ? ? ? ? ? ? ? ? ? ? ? ? ? 0 0 0 0 0 0 0 I M y F ? ? ? t h h k k , T T k k , , 0 0 0 0 0 y y F y C I I C Q ? C u M Q M y y q q q qq q u ? Convergence: When the value of residue (

) and corrections in equation (**??**9) is small, the GTSTIFF integrator in MSC Adams estimates local integration error which is a function of difference between the predicted and corrected value, step size h and the order of integration [29]. When this integration error is less than the specified integration error tolerance in MSC V.

16 Results and Discussions

The crawler track assembly in Figure 2 is modeled in SOLIDWORKS 2013 and the solid model is imported into MSC ADAMS. A 3-D virtual crawler track interacting with oil sands is created in MSC ADAMS to simulate the dynamic propel action of the crawler track for two types of motion constraints. It should be noted that before any propelling operation begins, the oil sand model along with crawler track is allowed to reach its static equilibrium position. From the equilibrium position, the simulation experiment for the 10s period of straight line and turning motion of crawler track on oil sand ground have been carried out to study the linear and angular motion of crawler track, contact forces between crawler shoes and ground and deflection of the oil sand terrain. In this paper, only the kinematics (displacement, velocity and accelerations) of crawler shoes are presented. The dynamic results (contact forces, constraint forces and total deformation of oil sand) are presented separately in the force part of this paper. The time variation of velocity of different crawler shoes in the x, y and z directions are shown in Figure 12. The x -velocity variation in Figure 12a shows that with the exception of part 14, all other shoes have fluctuating x -velocity variation in time during their translation motion. This is because the longitudinal driving constraint is only applied on part 14 while other crawler shoes x-velocity behavior are also influenced by external and joint forces. The lateral sliding velocity (yvelocity) is the same for all crawler shoes as shown in Figure 12b. The vertical velocity 23 (Figure 12c) also shows fluctuating behavior due to vertical bouncing of crawler track during its propelling motion. The accelerations of different crawler shoes in x, y and z-directions is shown in Figure 13. The acceleration of part 14 in the x-direction is dictated by the driving constraint (maximum acceleration on part 14 is 0.03 m/s2), while other parts have large fluctuations in their values as shown in Figure

13a. The magnitude of acceleration in the y-direction is much smaller in comparison to their values in z-direction as shown in Figures 13b and 13c Figure 14 shows the variation of angular velocities in x, y and z directions. It can be seen from Figure 14a that all crawler shoes have same angular velocity variation with time in x-direction and hence the whole crawler track rolls about the x-axis during its propeling motion. This rolling angular velocity attains its peak value when the crawler track attains its specified xtranslation velocity (Figure 12a) and decreases thereafter as shown in Figure 14a. The crawler shoes also rotates about y-axis (join t axis) with large varying angular velocity (Figure 14b) causing relative rotational motion between adjacent shoes of the crawler track. The crawler track also experiences small fluctuating rotational velocities along the global zdirection with average value approximately equal to zero as shown in Figure 14c. This rotation velocity causes crawler track to slide left or right from its direction of motion. 15a. Due to the fluctuating rotational velocity arising from equivalent revolute joint, the crawler shoes also have unsteady angular acceleration variation about yaxis (Figure 15b). The angular acceleration variation in zdirection (Figure 15c) shows that its average value is approximately zero and hence the crawler track will maintain its straight line motion. The time variation of velocities in x, y and z directions for crawler shoe 9 for the case of translation and turning motion is shown in Figure 17. The x-velocity variation show similar behavior for both motion types as shown in Figure 17a. The y-velocity (Figure 17b) shows large fluctuations during the middle of the turning motion when compared with translation motion type. This is due to the irregular increase in the lateral displacement of the crawler track (y-displacement in Figure 16b) when the crawler is turning at its prescribed The comparison of time variation of acceleration in x, y and z directions for crawler shoe 9 for both motion types reveal similar general behavior as shown for velocity distributions in Figure 17 and hence not plotted. The angular velocity variation for crawler shoe 9 is shown in Figure 18. The bouncing action of the crawler track also produces simultaneous rolling motion as shown by the angular velocity distribution about x-axis in Figure 18a. But turning motion exhibits increased rolling behavior when compared with translation motion due to the unsteady lateral sliding of the crawler track. The angular velocity in y-direction shows similar fluctuating behavior for both motion types while the angular velocity about z-axis for turning motion follows the rotation motion constraint (1.0 deg/s) imposed on the moving zaxis of the body fixed motion coordinate system on part 14. The angular acceleration comparison for both motion types also shows similar unsteady behavior as angular velocity (Figure 18) and hence not plotted here.

17 Conclusions

The dynamic equation of motion governing the multi-body model of crawler track assembly is obtained to study the propelling motion of crawler track on the oil sand terrain. A simple two-body contact dynamic problem is simulated in MSC Adams and the simulation results for accelerations and constraint forces at a given time is verified by solving the same problem analytically using the dynamic equations of motion and comparing the analytical solution to the simulation results. Subsequent to analytical verification, a rigid 3D virtual prototype model of the crawler track interacting with the oil sand terrain is developed and simulated in ADAMS environment. The simulation is carried out for the prescribed translation and rotation motion constraints on one of the crawler shoes in the track as reported in the kinematics part of this paper. The interaction between each crawler shoe and ground is modeled using contact force formulation in MSC ADAMS. The kinematic simulation results of the crawler track propelling on the ground for both driving constraints show that in 10 s the crawler slips forward for a maximum longitudinal distance of 0.75 m with vertical bouncing, lateral sliding and rotation about the x, y and z-axes. For translation motion, the maximum values of lateral sliding and vertical bouncing are 1 cm and 3.5 cm from the equilibrium position. The corresponding maximum sliding and bouncing velocities and accelerations are 0.06 m/s and 0.45 m/s and 1.8 m/s2 and 27 m/s2. The maximum magnitude of angular velocities and accelerations attained about the three orthogonal axes are 12.

[1] [2]

1

Figure 1: Figure 1 :

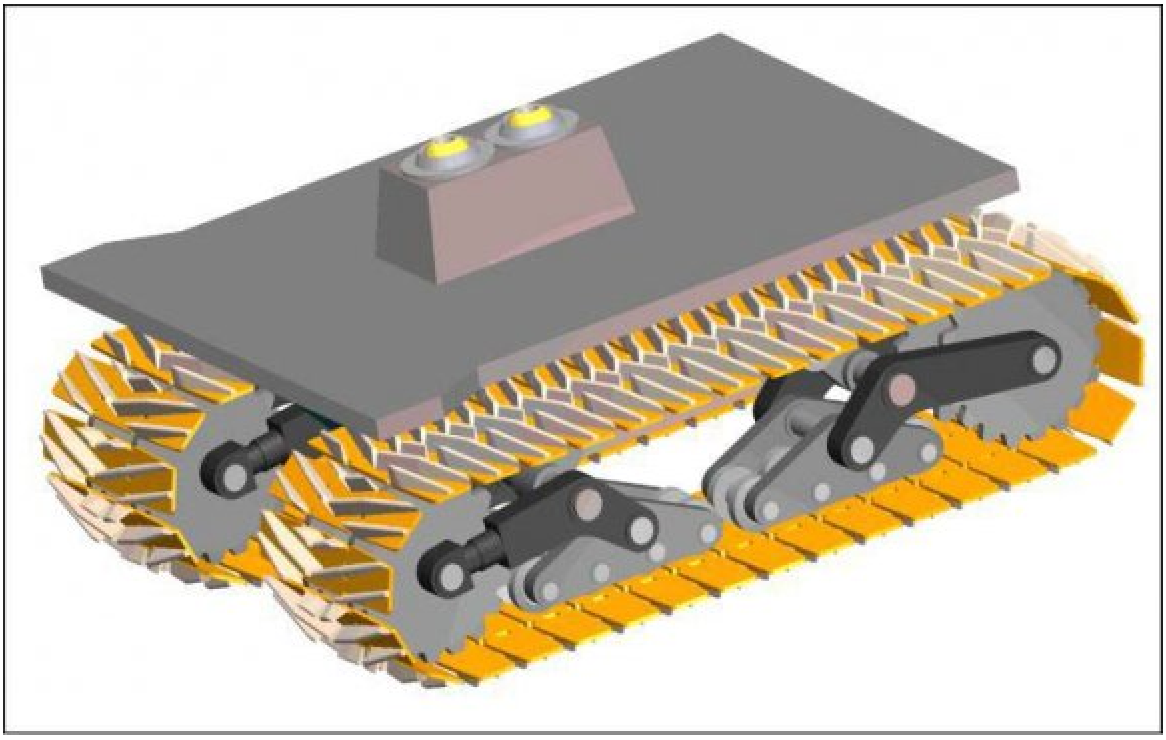

Figure 2:

2 

Figure 3: Figure 2 :

Figure 4:

Figure 5:

5 

Figure 6: Figure 5 :

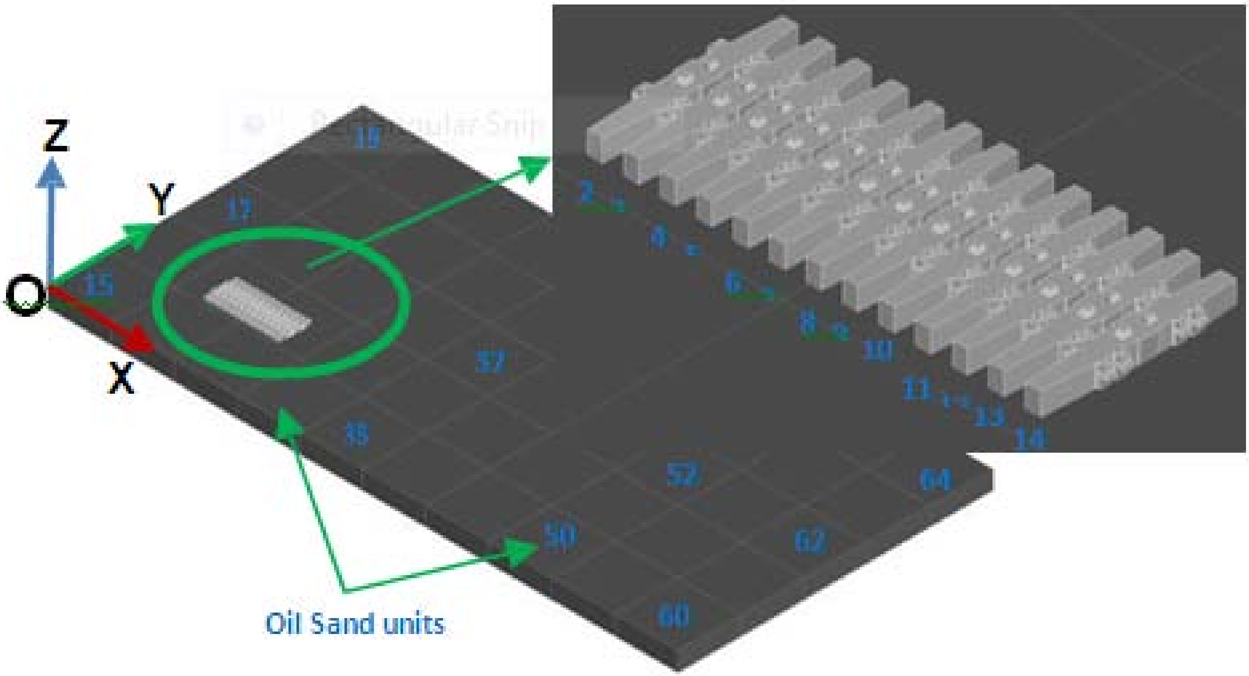

Figure 7: u

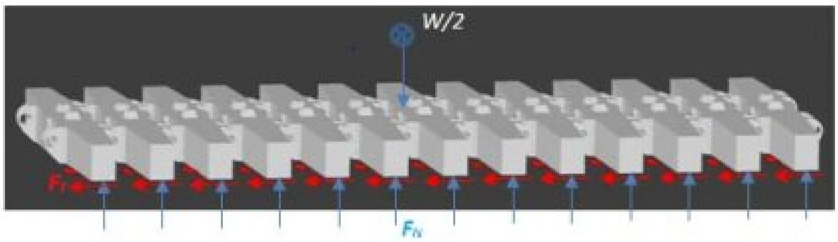

6

Figure 8: Figure 6 :

7 [redacted]

Figure 9: Figure 7 :

[redacted]

Figure 10: F

[redacted]

Figure 11:

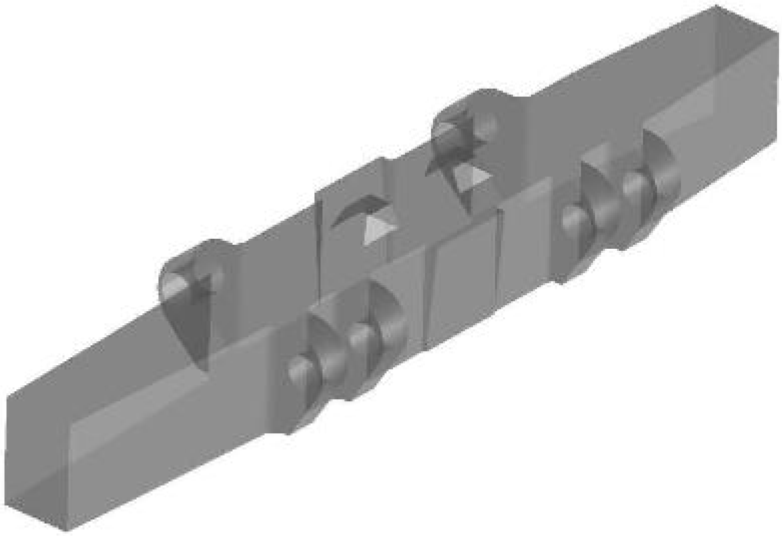

Figure 12:

8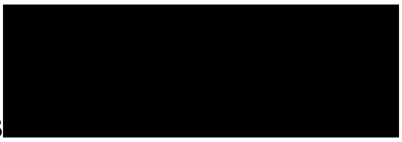

Figure 13: Figure 8 :

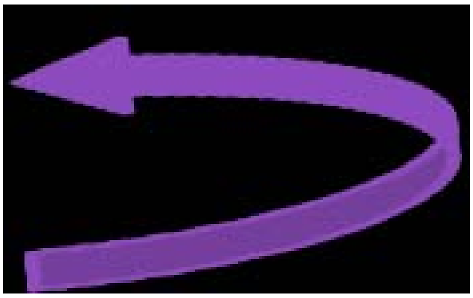

Figure 14: F

9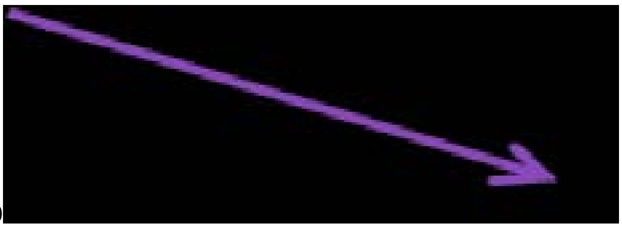

Figure 15: Figure 9 :

10

Figure 16: Figure 10 :

3

Figure 17: 3 3 M

15[redacted]

Figure 18: © 20 15

111[redacted]

Figure 19: Case 1 :Figure 11 :

12[redacted]

Figure 20: Figure 12 :

[redacted]

Figure 21:

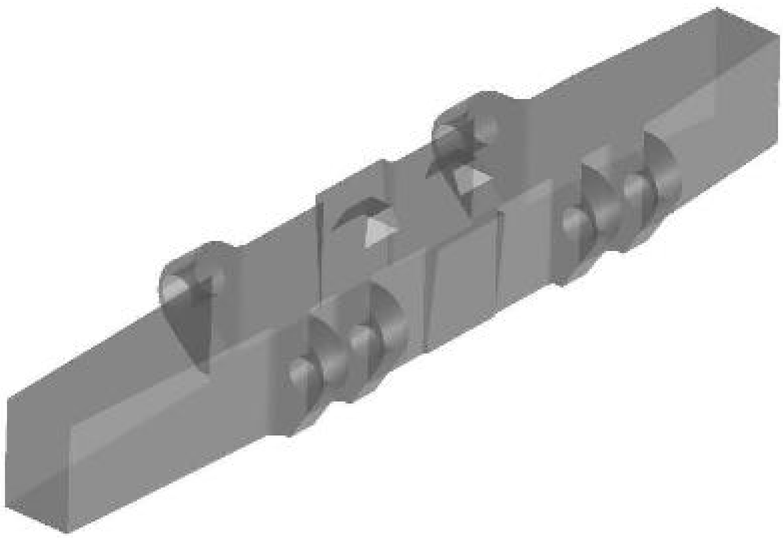

13

Figure 22: Figure 13 :

14[redacted]

Figure 23: Figure 14 :F

1516[redacted]

Figure 24: Figure 15 :Figure 16 :

17 

Figure 25: Figure 17 :

18 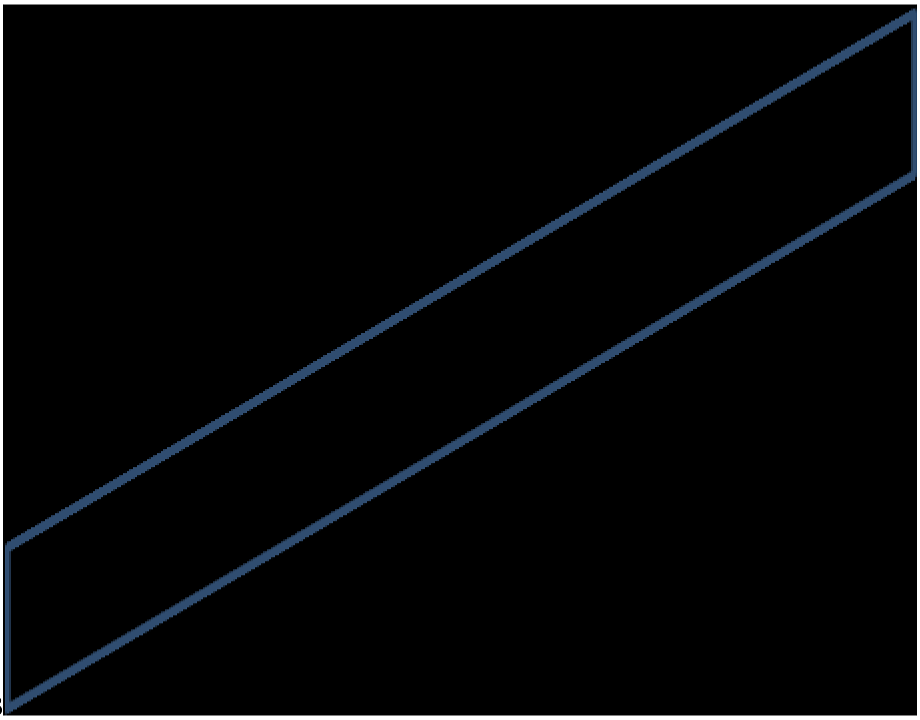

Figure 26: Figure 18 :

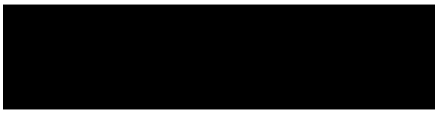

Figure 27:

1

Body	Density (kg/m 3)	Volume (m 3)	Mass (kg)
Crawler Shoe	7847.25	0.5966	4681.67
Oil-sand unit	1600.0	98.0	1.568 x 105

Figure 28: Table 1 :

2

Year 2015
20
Issue V Version I
e XV
F

[Note: Friction Parameters used in the study[28,29] © 2015 Global Journals Inc. (US)Global Journal of Researches in Engineering ( ) VolumMulti-Body Dynamic Modeling and Simulation of Crawler-Formation Interactions in Surface Mining Operations -Crawler Kinematics]

Figure 29: Table 2 :

3

[Note: Stiffness(k), (MN/m) Damping (c), (kN-s/m) Spring length (l o), (m) 20 120 5.0]

Figure 30: Table 3 :

5

Year 2015
25
XV Issue V Version I
Journal of Researches in Engineering ( ) Volume F
Global

Figure 31: Table 5 :

6

Tangential Force (N)

Figure 32: Table 6 :

7

Multi-Body Dynamic Modeling and Simulation of Crawler-Formation Interactions in Surface Mining
Operations -Crawler Kinematics
2
Body
2

Year 2015
Issue V Version I
e XV
( ) Volum F
Global Journal of Researches in Engineering

[Note: © 2015 Global Journals Inc. (US)]

Figure 33: Table 7 :

8

Figure 34: Table 8 :

9

Figure 35: Table 9 :

, , linearization of equation (52). Using first order Taylor's series, equation (??2) can be linearized about and at current time to obtain equations (??4) and (55).

[Joy Global Inc] , Joy Global Inc .

[Shabana ()] , A A Shabana . *Computational dynamics* 2010. John Wiley & Sons. (3rd Edition)

[4100C BOSS Electric Mining Shovel -AC Drive Product Overview ()] http://www.phmining.com/MinePro/Literature/Brochures/SUR_4100C_BOSS_AC_BRO_XS-5491.pdf *4100C BOSS Electric Mining Shovel -AC Drive Product Overview*, 2012. p. .

[Ryu et al. ()] 'A compliant track link model for high-speed, high-mobility tracked vehicles'. H S Ryu , D S Bae , J H Choi , A A Shabana . *Int. J. Numer. Meth. Engng* 2000. 48 p. .

[Rubinstein and Hitron ()] 'A detailed multibody model for dynamic simulation of off-road tracked vehicles'. D Rubinstein , R Hitron . *Journal of Terramechanics* 2004. 41 p. .

[Rubinstein and Coppock ()] 'A detailed single-link track model for multi-body dynamic simulation of crawlers'. D Rubinstein , A Coppock . *Journal of Terramechanics* 2007. 44 p. .

[Ma and Perkins ()] 'A hybrid track model for studying dynamic track/sprocket Contact'. Z D Ma , N C Perkins . *Proceedings of the ASME Noise Control and Acoustics Division*, (the ASME Noise Control and Acoustics Division) 1999. p. .

[Bedford and Fowler ()] A Bedford , W Fowler . *Eng. Mechanics: Statics and Dynamics*, 2002. Prentice Hall.

[Edward ()] 'Computer aided kinematics and dynamics of mechanical systems'. J H Edward . *Allyn and Bacon Series in Engineering* 1989.

[Nakanishi and Shabana ()] 'Contact forces in the nop-linear dynamic anlysis of tracked vehicles'. T Nakanishi , A A Shabana . *Int. J. for Numerical Methods in Engineering* 1994. 37 p. .

[Nakanishi and Shabana ()] 'Contact forces in the nop-linear dynamic anlysis of tracked vehicles'. T Nakanishi , A A Shabana . *Int. J. for Numerical Methods in Engineering* 1994. 37 p. .

[Frimpong et al. ()] 'Dynamic torque and soil deformation mechanics and simulation of the GAP machinery'. S Frimpong , Y Li , R Suglo . *J Powder Metall Min* 2013. 1 p. 2.

[Shabana ()] *Dynamics of multi-body Systems*, A A Shabana . 1998. Cambridge Univ. Press. (2nd Edition)

[Hibbeler ()] *Engineering mechanics, dynamics*, R C Hibbeler . 1989. Macmillan. (5th Edition)

[Madsen ()] *High fidelity modeling and simulation of tracked elements for off-road applications using MSC/ADAMS*, J Madsen . 2007.

[Lee et al.] H C Lee , J H Choi , A A Shabana . *Spatial dynamics of multi-body tracked vehicles Part II: Contact forces and simulation results*,

[Frimpong et al. ()] 'Mechanics of cable shovel-formation interactions in surface mining excavations'. S Frimpong , Y Hu , K Awuah-Offei . *Journal of Terramechanics* 2005. 42 p. .

[Ferrati and Girelli ()] 'Modeling and simulation of an agricultural tracked vehicle'. G Ferrati , R Girelli . *Journal of Terramechanics* 1999. 36 p. .

[Lindberg ()] *MSC Adams modeling of mechanical system in A400M crew Entrance Door*, D Lindberg . 2012. Sweden. Linkoping Institue of Technology (Master Thesis)

[Msc ()] *MSC ADAMS/Solver help document. © MSC Corporation*, Msc . 2014. San Diego, CA.

[Msc ()] *MSC ADAMS/View help document. © MSC Corporation*, Msc . 2014. San Diego, CA.

[Schiehlen et al. ()] 'Multibody dynamics in computational mechanics and engineering applic'. W Schiehlen , N Guse , R Seifried . *Comput. Methods Appl. Mech. Engrg* 2006. 195 p. .

[Kong et al. (2008)] 'Nonlinear contact analysis of gear teeth for malfunction diagnostics'. D Kong , J M Meagher , C Xu , X Wu , Y Wu . *Proceedings of the IMAC 26th Conference on Structural Dynamics*, (the IMAC 26th Conference on Structural DynamicsOrlando, Fla, USA) February, 2008.

[Ph ()] *Peak Performance Practices: Lower Works, © P&H MinePro*, P&h . 2005. Milwaukee, WI.

[Frimpong and Thiruvengadam ()] *Rigid multi-body kinematics of shovel crawler-formation interaction*, S Frimpong , M Thiruvengadam . 2015. (Submitted to Engineering Failure Analysis.___)

[Lee et al. ()] 'Spatial dynamics of multi-body tracked vehicles II: Contact forces and simulation'. H C Lee , J H Choi , A A Shabana . *Vehicle Systems Dynamics* 1998. 29 p. .

[Choi et al.] *Spatial dynamics of multibody tracked vehicles Part I: Spatial equations of motion*, J H Choi , H C Lee , A A Shabana .

[Choi et al. ()] 'Spatial dynamics of multibody tracked vehicles. Part I: Spatial equations of motion'. J H Choi , H C Lee , A A Shabana . *Vehicle Systems Dynamics* 1998. 29 p. .

[Frimpong and Li ()] 'Stress loading of the cable shovel boom under in-situ digging conditions'. S Frimpong , Y Li . *Engineering Failure Analysis* 2007. 14 p. .

[Wong ()] J Y Wong . *Theory of Ground Vehicles*, 2001. John Wiley & Sons, Inc. (3rd Edition)